Supporting Information

Even Hard Sphere Colloidal Suspensions Display Fickian yet Non-Gaussian Diffusion

Juan Guan,[a] *Bo Wang,*[a] *and Steve Granick*[a,b,c,*]

Departments of Materials Science,[a] Chemistry,[b] and Physics,[c] University of Illinois, Urbana, IL 61801

*Corresponding author: sgranick@illinois.edu

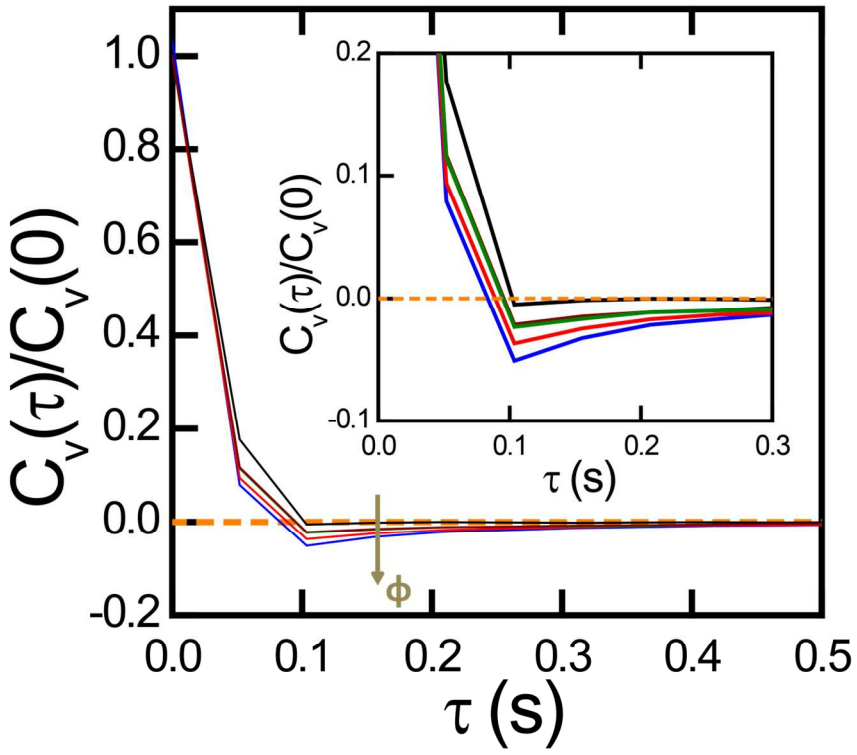

Figure S1. Velocity autocorrelation function $C_v(\tau)$ plotted against time lag τ on linear scales, where $C_v^{(\varepsilon)}(\tau) = \frac{1}{\varepsilon^2} < (x(\tau+\varepsilon) - x(\tau))(x(\varepsilon) - x(0)) >$ and here x is instantaneous nanoparticle position, τ is the delay time, and ε =0.05 s. A slight anti-correlation at 0.1 s quickly decays to 0. The anti-correlation increases slightly with increasing volume fraction. Colors indicate □=0 (black), □=0.15 (brown), □=0.30 (green), □=0.45 (red), □=0.55 (blue). (Inset) a magnified view of the anti-correlation region.

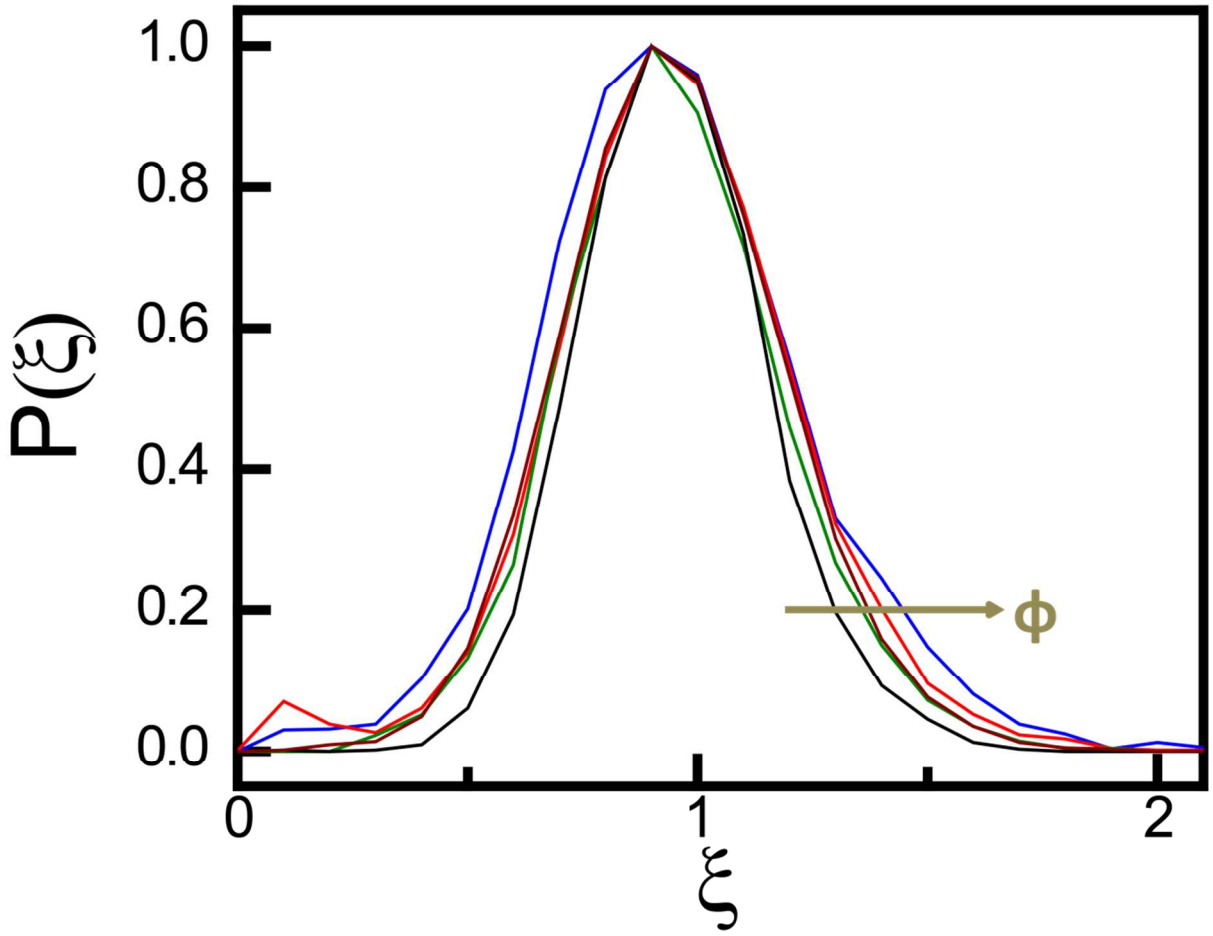

Figure S2. The distribution of ergodic breaking parameter ξ defined in reference 1. Checking for dynamic heterogeneity by inspecting the time-averaged mean square displacement (MSD) of individual trajectories, we calculated the ratio of MSD of individual trajectories to the ensemble average, specifically $\xi \equiv \frac{\overline{\delta^2(\Delta,\tau)}}{<\overline{\delta^2(\Delta,\tau)}>}$ where $\overline{\delta^2(\Delta,\tau)} = \frac{1}{\tau-\Delta}\int_0^{\tau-\Delta}[r(t+\Delta)-r(t)]^2 dt$, and $<\cdots>$ denotes ensemble average. Here $\tau = 3.3\,\mathrm{s}$ and $\Delta = 0.1\,\mathrm{s}$, where τ denotes how long each trajectory lasts and is selected to be sufficiently long to ensure the accuracy of ξ but sufficiently short that the distribution of ξ can be calculated from many trajectories. The symbol Δ is the time interval

used to calculate MSD to reflect the dynamic spread. Note the slight tendency for the distribution of ξ to broaden with increasing volume fraction. Colors: same as in Figure S1.

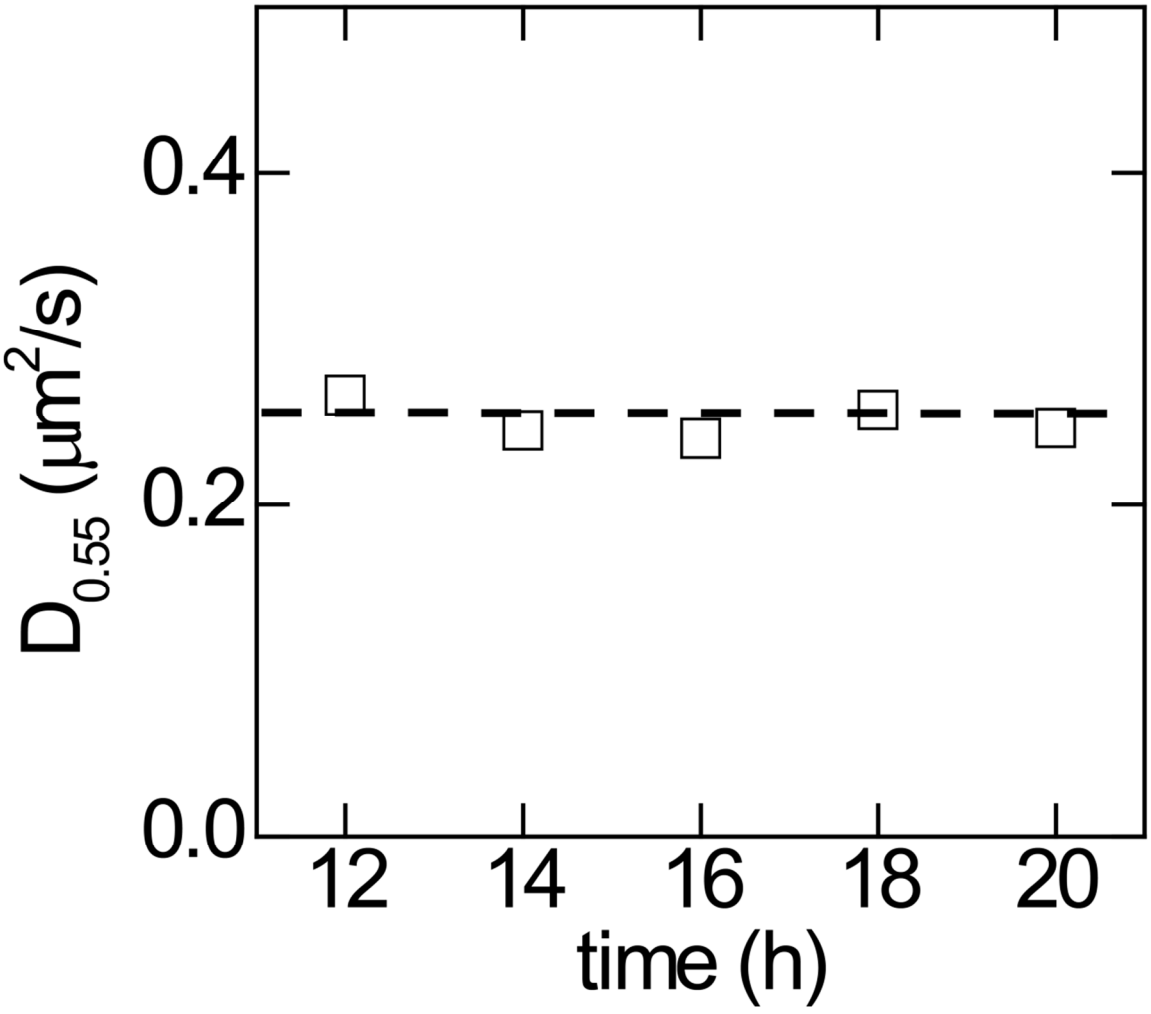

Figure S3. No aging or change of mobility was observed for the sample at □=0.55. This sample was pre-equilibrated for 12 hrs on the microscope stage before the experiment, then measurements were made for an additional 8 hrs. The dashed line shows the ensemble-averaged diffusivity.

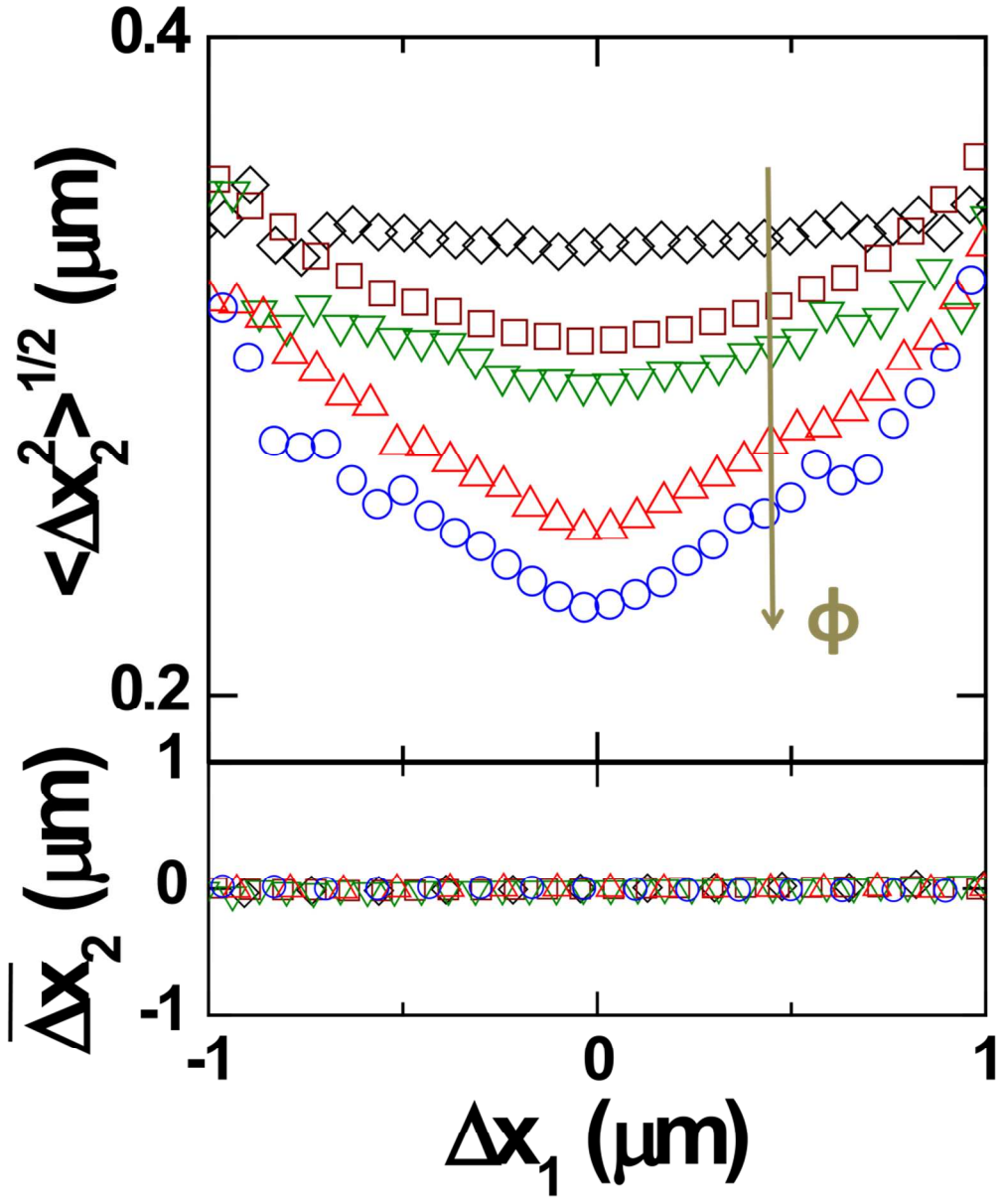

Figure S4. Conditional displacement of successive time intervals. The abscissa is displacement in the first time interval. (Upper panel) The ordinate is root mean square displacement in the second time interval. The U-shaped pattern centered around zero displacement, observed in the presence of matrix particles but not in pure solvent, shows that large displacements are likely followed by large displacements in the presence of matrix particles. This trend grows with increasing volume fraction. Time interval is 0.1 s for each □. (Lower panel) The ordinate, mean

displacement in the second time interval, equals zero regardless of volume fraction. Time interval is 0.2 s (□=0, black), and 0.1 s otherwise. Colors indicate □=0.15 (brown), □=0.30 (green), □=0.45 (red), □=0.55 (blue).

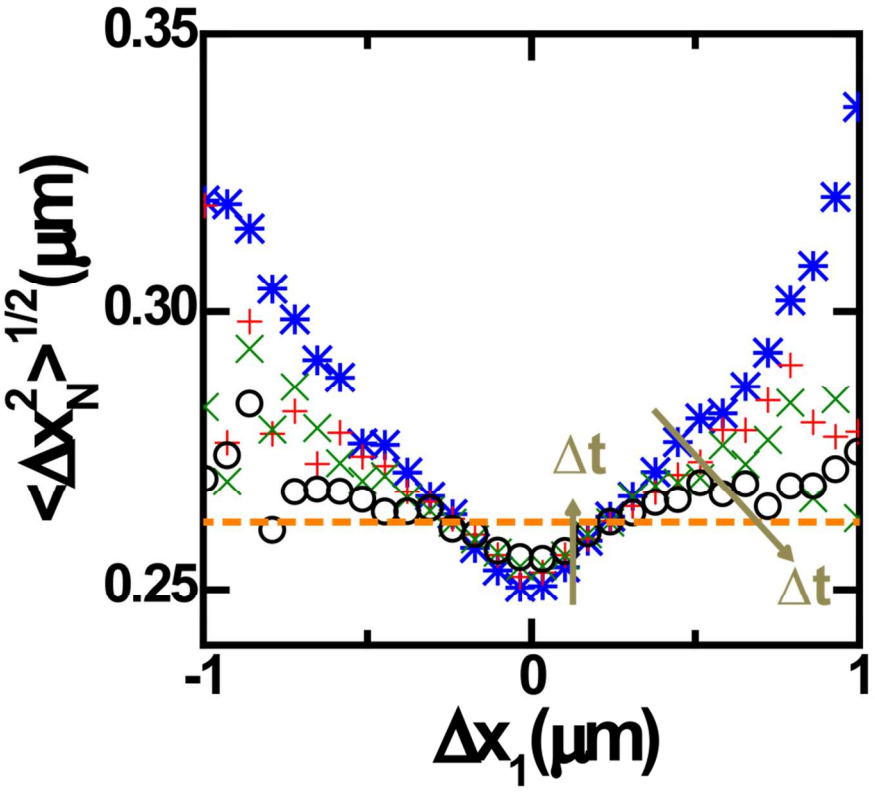

Figure S5. Conditional displacement of the Nth step given the displacement of the 1st step, with successive time intervals of 0.1 s and N up to a maximum of 10, at volume fraction □=0.45. The U-shaped pattern flattens slowly with increasing N. The horizontal dashed line shows the expected displacement value for zero correlation, calculated from the mean square displacement at this time. The data are plotted for N=2 (*), 3 (+), 4 (×), and 10 (○) corresponding to a lag time of 0.1 s, 0.2 s, 0.3 s, and 0.9 s respectively.

Table S1.

φ	mean surface distance between matrix particles (μm)*	$t_{collision}$ (s)**	$t_{transit}$ (s)$^{+}$	$l_{transit}$ (μm)$^{\#}$
15%	**2**	**6**	**1.0**	**1.0**
30%	**1.1**	**2**	**1.0**	**0.9**
45%	**0.7**	**0.8**	**0.6**	**0.6**
55%	**0.5**	**0.4**	**0.4**	**0.4**

* estimated from inter-particle distance between matrix particles at a given φ.

** estimated from mean surface distance and probe diffusivity in solvent.

$^{+,\#}$ estimated from Figure 1b.

Estimate of timescales

From data in the literature, the sub-diffusive to diffusive transition for matrix particles of this same size at volume fraction 0.45 occurs at ~100 s.[2] Also from literature, the time for a matrix particle to diffuse its own size at □=0.45 is estimated to be ~100 s.[3] We identify this timescale with the longest relaxation timescale of the matrix. Because the matrix particles diffuse so slowly and are obstructed by their neighbors, over our experimental window of <10 s the matrix structure would not significantly rearrange. For example, movie S2 shows Brownian motion of matrix particles at □=0.30.

Inspection of the velocity autocorrelation function implies that collision and back scattering events occur on the time scale ~0.1 s (Figure S1). Analysis of the mean-square displacement

implies that the transition time from diffusion to sub-diffusion in this interstitial diffusion process is ~1 s (Figure 1b). This longer time is reasonable physically, as the transition should require several collision and back scattering events. In fact, the implied length scale is calculated to be roughly the average surface distance between matrix particles at the respective volume fractions (Table S1).

Movie captions

Movie S1. Video of tracer Brownian motion taken using epifluorescence microscopy. The 0.28 μm diameter tracer particles are mixed into a suspension of larger 2.2 μm diameter matrix particles at volume fraction □=0.55 and hard sphere interactions. The movie plays in real time. The field of view is 80×80 μm^2.

Movie S2. Video of matrix particle diffusion, which is far slower than diffusion of smaller tracer particles. The 3 μm matrix particles are fluorescently labeled. The suspension has □=0.30. The movie is taken using HILO microscopy, which is a light sheet microscopy that illuminates a thin layer a few microns removed from the surface.[4] The movie plays in real time. The field of view is 45×45 μm^2.

References

[1] Burov, S.; Jeon, J.-H.; Metzler, R.; Barkai, E., Single Particle Tracking in Systems Showing Anomalous Diffusion: the Role of Weak Ergodicity Breaking. *Phys. Chem. Chem. Phys.* **2011**, *13*, 1800-1812.

[2] Weeks, E. R.; Crocker, J. C.; Levitt, A. C.; Schofield, A.; Weitz, D. A., Three-Dimensional Direct Imaging of Structural Relaxation Near the Colloidal Glass Transition. *Science* **2000**, *287*, 627-631.

[3] Kegel, W. K.; van Blaaderen, A., Direct Observation of Dynamical Heterogeneities in Colloidal Hard-Sphere Suspensions. *Science* **2000**, *287*, 290-293.

[4] Tokunaga, M.; Imamoto, N.; Sakata-Sogawa, K., Highly Inclined Thin Illumination Enables Clear Single-Molecule Imaging in Cells. *Nature Met.* **2008**, *5*, 159-161.